Available online at www.sciencedirect.com

ScienceDirect

Nuclear Physics A 982 (2019) 671–674

www.elsevier.com/locate/nuclphysa

XXVIIth International Conference on Ultrarelativistic Nucleus-Nucleus Collisions (Quark Matter 2018)

Measurements of directed and elliptic flow for D^0 and $\overline{D^0}$ mesons using the STAR detector at RHIC

Subhash Singha (for the STAR Collaboration) [1]

Department of Physics, Kent State University, Ohio 44242, USA

subhash@rcf.rhic.bnl.gov

Abstract

We report on the first evidence for a non-zero rapidity-odd directed flow (v_1) for D^0 and $\overline{D^0}$ mesons in 10-80% centrality Au+Au collisions at $\sqrt{s_{\rm NN}}$ = 200 GeV measured with the STAR detector at RHIC. The slope of the v_1 rapidity dependence (dv_1/dy) averaged over D^0 and $\overline{D^0}$ mesons is -0.081 ± 0.021 ± 0.017, while that of charged kaons is -0.0030 ± 0.0001 ± 0.0002, suggesting significantly larger slope for the D^0 mesons. Models indicate that the large dv_1/dy of D^0 mesons is sensitive to the initially tilted source. We also present a new measurement of the D^0 meson elliptic flow (v_2) as a function of transverse momentum (p_T) in Au+Au collisions at $\sqrt{s_{\rm NN}}$ = 200 GeV with an improved precision with respect to the previously published results.The D^0 v_2 results are compared to those of light-flavor hadrons to test the number-of-constituent-quark (NCQ) scaling. Both the v_1 and v_2 results are compared to recent hydrodynamic and transport model calculations.

Keywords: relativistic heavy-ion collisions, heavy flavor, directed flow, elliptic flow

1. Introduction

Heavy quarks play a crucial role in probing the Quark Gluon Plasma (QGP) phase because their masses are significantly larger than the typical temperature achieved in the medium. The production of heavy quarks occurs mainly during the primordial stage of heavy-ion collisions before the QGP is formed. As a consequence, they experience the entire evolution of the system and can be used to access information concerning the early time dynamics [1]. A recent hydrodynamic model [2], which incorporates Langevin dynamics for heavy quarks combined with an initial tilt of the source [3], predicts a relatively larger v_1 for heavy flavors compared to the light ones. The model demonstrates the sensitivity of the D-meson v_1 slope to the initially tilted geometry and the interaction between charm quarks and the medium. Furthermore, another model [4] predicts that the transient electromagnetic (EM) field generated in heavy-ion collisions can induce

[1] A list of members of the STAR Collaboration and acknowledgements can be found at the end of this issue. S.S. acknowledges financial support from DOE project (Grant No. DE-FG02-89ER40531), USA.

https://doi.org/10.1016/j.nuclphysa.2018.09.010

opposite v_1 for charm (c) and anti-charm ($\bar{c}$) quarks. Such an EM-field-induced v_1 for hadrons containing heavy quarks is predicted to be several orders of magnitude larger than that for light-flavor hadrons [5]. Thus, the separate measurement of v_1 for D^0 and $\overline{D^0}$ can offer insight into the early-time EM fields.

Recent measurements at RHIC, based on 2014 data, have shown that D^0 mesons in minimum-bias and mid-central heavy-ion collisions exhibit significant elliptic flow [6]. The flow magnitude follows the same number-of-constituent-quark (NCQ) scaling pattern as observed for light-flavor hadrons in mid-central collisions. It is of particular interest to measure the centrality dependence of these observables and to test the NCQ scaling for charmed hadrons in different centrality classes. During 2016, STAR [7] collected an additional sample of Au+Au collisions at $\sqrt{s_{\rm NN}}$ 200 GeV using the Heavy Flavor Tracker (HFT) [8, 9] detector. An improved precision for the anisotropic flow measurements of heavy-flavor hadrons has been achieved by combining the data samples collected during 2014 and 2016 allowing more quantitative studies of the QGP properties.

2. Analysis details

Minimum-bias events are defined by a coincidence of signals in the east and west Vertex Position Detectors (VPD) [10] located at pseudorapidity $4.4 < |\eta| < 4.9$. The collision centrality is determined from the number of charged particles within $|\eta| < 0.5$ and corrected for triggering efficiency using a Monte Carlo Glauber simulation [11]. The D^0 and $\overline{D^0}$ mesons are reconstructed via their hadronic decay channels: $D^0\,(\overline{D^0}) \rightarrow K^-\pi^+\,(K^+\pi^-)$ (branching ratio: 3.89%, $c\tau \sim 123\ \mu$m) [12] by utilizing the Time Projection Chamber (TPC) [13] along with the HFT. Good-quality tracks with $p_T > 0.6$ GeV/c and $|\eta| < 1$ are ensured by requiring a minimum of 20 TPC hits (out of possible 45), and with at least one hit in each layer of the Intermediate Silicon Tracker (IST) and PiXeL (PXL) components of the HFT [6]. The identification of D^0 decay daughters is based on the specific ionization energy loss (dE/dx) in the TPC and on the velocity of particles ($1/\beta$) measured by the Time of Flight (TOF) [14] detector. To reduce the background and enhance the signal-to-background ratio, topological variable cuts are optimized using the Toolkit for Multivariate Data Analysis (TMVA) package [15, 6]. The first-order event plane azimuthal angle (Ψ_1) is reconstructed using the Zero-Degree Calorimeter Shower Maximum Detectors (ZDC-SMDs) [16]. The ZDC-SMDs ($|\eta| > 6.3$) are separated by about five units in pseudo rapidity from the TPC and the HFT. This separation reduces significantly the possible non-flow effects in v_1 measurements. The second-order event plane (Ψ_2) is reconstructed from tracks measured in the TPC. To suppress the non-flow effects in the v_2 measurements, only tracks that are in the opposite rapidity hemisphere with at least $\Delta\eta > 0.05$ with respect to the reconstructed D^0, are employed for the Ψ_2 reconstruction. The v_1 and v_2 coefficients are calculated using the event-plane method [17] measuring the D^0 yields in different azimuthal intervals defined with respect to the event plane angle ($\phi - \Psi_n$). The D^0 yields are weighted by the inverse of the reconstruction efficiency × acceptance for each interval of collision centrality. The observed v_n is then calculated by fitting the azimuthal dependence of the D^0 yield using the function $p_0(1 + 2\, v_n^{\rm obs} \cos[n\,(\phi - \Psi_n)])$. The resolution-corrected v_n is then obtained by dividing $v_n^{\rm obs}$ by the event-plane resolution corresponding to Ψ_n [18].

3. Results

The left panel in Fig. 1 presents the rapidity-odd directed flow for D^0 and $\overline{D^0}$ mesons and their average in 10-80% central Au+Au collisions at $\sqrt{s_{\rm NN}} = 200$ GeV with $p_T > 1.5$ GeV/c using 2014 and 2016 data combined. The $v_1(y)$ slope for D^0 mesons is extracted by fitting the data with a linear function constrained to pass through the origin. The choice of using a linear function is driven by the limited D^0 statistics. The observed dv_1/dy for D^0 and $\overline{D^0}$ is -0.102 ± 0.030 (stat.) ± 0.021 (syst.) and -0.061 ± 0.030 (stat.) ± 0.023 (syst.), respectively, while dv_1/dy for their average is -0.081 ± 0.021 (stat.) ± 0.017 (syst.), corresponding to a 3σ significance. The heavy flavor results are compared to the average of K^+ and K^- [19]. The kaon v_1 slope is obtained from a similar linear fit, and the fitted dv_1/dy for kaons is -0.0030 ± 0.0001 (stat.) ± 0.0002 (syst.). While the sign of dv_1/dy is the same, the magnitude of D^0 dv_1/dy is about 20 times larger (2.9σ significance) compared to the kaon dv_1/dy. A recent hydrodynamic model [2] predicts that the drag

from the initially tilted bulk can induce a relatively larger v_1 for heavy-flavor hadrons compared to light hadron species. Hence, the D meson v_1 slope can be used to probe the initial thermal matter distribution in the longitudinal and transverse directions. Furthermore, the initial EM field can induce opposite v_1 for charm and anti-charm quarks. A hydrodynamic model calculation combined with initial EM fields suggests that the v_1 splitting due to the EM field can be smaller than the v_1 induced by the drag of the tilted bulk [20]. The dashed magenta line in the left panel of Fig. 1 represents the $v_1(y)$ prediction from this hydrodynamic model incorporating the initial EM field [20]. The model predicts the correct sign for both D^0 and $\overline{D^0}$ mesons, but the magnitude of v_1 is underestimated when using the particular choice of model parameters in Ref. [20]. The difference in v_1 (Δv_1) between the D^0 and $\overline{D^0}$, predicted to be sensitive to the initial EM field, is presented in the right panel of Fig. 1. The D^0 results are compared with two model predictions, shown by solid blue [4] and magenta dashed [20] lines. The current precision of the data does not permit firm conclusions concerning the difference and ordering between the D^0 and $\overline{D^0}$ mesons. The

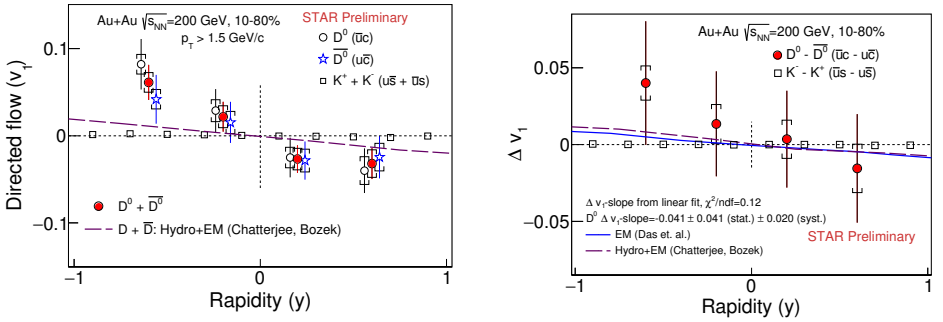

Fig. 1. (Color online) Left panel: Open circle and star markers present D^0 and $\overline{D^0}$ v_1 as a function of rapidity for p_T >1.5 GeV/c in 10-80% Au+Au collisions at $\sqrt{s_{\rm NN}}$ = 200 GeV, while the solid red circles are their average. The D^0 and $\overline{D^0}$ data points are shifted along the horizontal axis by ± 0.04 for visibility. Open black squares present $v_1(y)$ for charged kaons [19]. The magenta dashed line shows $v_1(y)$ from a hydro model calculation incorporating the initial electromagnetic field [20]. Right panel: Solid red symbols present the difference between D^0 and $\overline{D^0}$, while the open black squares are the difference between K^- and K^+. The solid blue and magenta dashed lines are the Δ v_1 prediction from Refs. [4] and [20], respectively. In both panels, the vertical bars and caps denote statistical and systematic uncertainties, respectively.

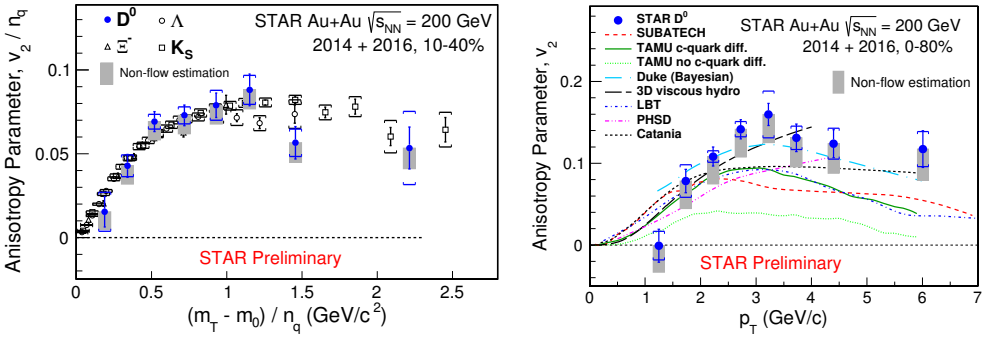

Fig. 2. (Color online) Left panel: v_2/n_q as a function of $(m_T - m_0)/n_q$ for D^0 and $\overline{D^0}$ mesons combined in 10-40% central Au+Au collisions at $\sqrt{s_{\rm NN}}$ = 200 GeV along with K^0_S, Λ, and Ξ [21]. Right panel: v_2 as a function of p_T for D^0 and $\overline{D^0}$ mesons combined in 0-80% Au+Au collisions compared with model calculations [22, 23, 24, 25, 26, 27, 28].

averaged $v_2(p_T)$ of D^0 and $\overline{D^0}$ mesons is measured in 0-10%, 10-40% and 0-80% central Au+Au collisions at $\sqrt{s_{\rm NN}}$ = 200 GeV based on combined datasets recorded during 2014 and 2016. This provides about a 30% improvement in the statistical precision compared to previously published results using 2014 data alone [6]. The new results allow us to perform improved NCQ-scaling tests. The blue solid markers in the left panel of Fig. 2 present the NCQ-scaled v_2 as a function of NCQ-scaled transverse kinetic energy $(m_T - m_0)$ for D^0

mesons in 10-40% central Au+Au collisions at $\sqrt{s_{\rm NN}}$ = 200 GeV. The results are compared to light hadron species, namely the K^0_S meson and the Λ and Ξ baryons [21]. The NCQ-scaled D^0 v_2 is compatible within uncertainties with those of light hadrons for $(m_T - m_0)/n_q < 2.5$ GeV/c^2. This observation suggests that the charm quarks exhibit the same strong collective behavior as light-flavor quarks, and may be close to thermal equilibrium with the medium in Au+Au collisions at $\sqrt{s_{\rm NN}}$ = 200 GeV. The right panel in Fig. 2 presents the D^0 v_2 results in 0-80% central Au+Au collisions, and compared to SUBATECH [22], TAMU [23], Duke [24], 3D viscous hydro [25], LBT [26], PHSD [27], and Catania [28] model calculations. These models include different treatments of the charm quarks interactions with the medium and they also differ in their initial state conditions, QGP evolution, hadronization, etc. We have performed a statistical significance test of the consistency between the data and each model, quantified by χ^2/NDF and the p value. We have found that the TAMU model without charm quark diffusion cannot describe the data, while the same model with charm quark diffusion turned-on shows better agreement. All the other models can describe the data in the measured p_T region.

4. Conclusion

In summary, we report on the first evidence for a non-zero rapidity-odd directed flow of D^0 and $\overline{D^0}$ mesons in Au+Au collisions at $\sqrt{s_{\rm NN}}$ = 200 GeV in the 10-80% centrality class. The dv_1/dy of the average of D^0 and $\overline{D^0}$ mesons is -0.081 ± 0.021 ± 0.017, which is significantly larger than that of the charged kaons having dv_1/dy of -0.0030 ± 0.0001 ± 0.0002. Models indicate that the large dv_1/dy of D^0 is sensitive to the initially tilted source. However, the current precision of the data is not sufficient to clearly determine the difference and ordering between D^0 and $\overline{D^0}$ mesons, which, according to models, is sensitive to the initial electromagnetic field. We also report on the elliptic flow as a function of p_T for combined D^0 and $\overline{D^0}$ mesons combining 2014 and 2016 data samples. The D^0 v_2 result suggests that the charm quark may be close to thermal equilibrium with the medium. Furthermore, studies are now in progress in determining the D^0 v_2 in the peripheral collisions (40-80%), with an enlarged pseudorapidity gap to reduce non-flow effects.

References

[1] R. Rapp and H. van Hees arXiv:0803.0901
[2] S. Chatterjee and P. Bozek, Phys. Rev. Lett. **120**, 192301 (2018).
[3] P. Bozek and I. Wyskiel, Phys. Rev. C **81**, 054902 (2010).
[4] S. Das *et al.*, Phys. Lett. **B 768**, 260 (2017).
[5] U. Gursoy *et al.*, Phys. Rev. C **89**, 054905 (2014).
[6] L. Adamczyk *et al.* (STAR Collaboration), Phys. Rev. Lett. **118**, 212301 (2017).
[7] K. H. Ackermann *et al.*, Nucl. Instr. Meth. A **499**, 624 (2003).
[8] D. Beavis *et al.*, The HFT Technical Design report as prepared for the July 2011 CD2-3 review, STAR Note SN0600.
[9] G. Contin *et al.*, Nucl. Instr. Meth. A (in press); https://doi.org/10.1016/j.nima.2018.03.003.
[10] W. J. Llope *et al.*, Nucl. Instrum. Meth. A**522**, 252 (2004).
[11] B. Abelev *et al.*, (STAR Collaboration), Phys. Rev. C **79**, 034909 (2009).
[12] Review of Particle Physics, M. Tanabashi *et al.*, Phys. Rev. D **98**, 030001 (2018).
[13] M. Anderson *et al.*, Nucl. Instr. Meth. A **499**, 659 (2003).
[14] B. Bonner *et al.*, Nucl. Instr. Meth. A **508**, 181 (2003).
[15] A. Hocker *et al.*, PoS ACAT, **040** (2007).
[16] G. Wang, PhD thesis, Kent State University, 2006; https://drupal.star.bnl.gov/STAR/theses.
[17] A. M. Poskanzer and S. A. Voloshin, Phys. Rev. C **58**, 1671 (1998).
[18] H. Masui *et al.*, Nucl. Instrum. Meth. A **833**, 181 (2016).
[19] L. Adamczyk *et al.* (STAR collaboration), Phys. Rev. Lett. **120**, 062301 (2018).
[20] S. Chatterjee and P. Bozek, arXiv:1804.04893.
[21] B. I. Abelev *et al.*, (STAR collaboration), Phys. Rev. C **77**, 054901 (2008).
[22] T. Song *et al.*, Phys Rev C **92**, 014910 (2015).
[23] M. He. *et al.*, Phys Rev C **86**, 014903 (2012); Phys Rev Lett **110**, 112301 (2013).
[24] S. Cao *et al.*, Phys. Rev. C **97**, 014907 (2018).
[25] L. Pang *et al.*, Phys Rev C **86**, 024911 (2012).
[26] S. Cao *et al.*, Phys Rev C **94**, 014909 (2016).
[27] T. Song *et al.*, Phys Rev C **92**, 014910 (2015)
[28] F. Scardina *et al.*, Phys Rev **96**, 044905 (2017).